

OPTICAL ANALYSIS OF A HEMISPHERIC CONCENTRATOR WITH A MANUAL TRACKING SYSTEM FOR THE DECLINATION

KY, THIERRY S. M., KAM, SIÉ., DIANDA, BOUREIMA AND BATHIEBO, D. JOSEPH

(Received 29 April 2015; Revision Accepted 17 August 2015)

ABSTRACT

We present in this paper, a craft prototype of a fixed hemispheric concentrator, built from small square mirrors with a moon crescent receiver. The position of the receiver is adjusted every three days taking into account the declination. This system achieves a geometric mean concentration of 122 and the experimental measurements lead to temperatures varying between 120°C and 260°C in the plan for the least diffusion. The proposed improvements should allow for more competitiveness and convenience than the *Scheffler* system with its electromechanical sun tracking.

KEYWORDS: hemispheric concentrator, Fixed Mirror Distributed Focus – FPDF, Solar bowl, Scheffler,

INTRODUCTION

There are a number of difficulties associated with the use of solar systems in cooking food due to the target temperature: when it comes to solar ovens which need to reach temperatures from 250°C to 300°C for the baking of bread for example, it is necessary to use concentrators with sun tracking systems. Nowadays two systems of concentration prevail in solar cooking:

The "Scheffler" system (Munir *et al.*, 2010): Its reflector is a portion of a paraboloid with a pivot axis that passes through the focal point and the centre of this portion. This axis is the axis of rotation of the reflector for tracking the sun from east to west. As for the declination, (variation), it needs a setting-up every 2-3 days for the position and shape of the reflector. Finally, the Scheffler reflector has only a geometric mean concentration of 150 (Sardeshpande Pillai, 2012, P.221). Its apparently simple adjustment proves addictive for employees in Africa (Kombasséré, 2008).

The Central Collector (Quoilin, 2007) consists of a multitude of small squares or rectangular flat panels called heliostats independently activated which reflect on a common point target. For these collectors that promote energy at all costs, monitoring the sun-tracking system for each panel is different from one panel to another because of the geographical position of each element relative to the target. Chasing the sun does not consist in aligning the normal of each item with the incident ray, but rather to reflect this incident beam

towards the common target, a complex and sophisticated system involving robotics, managed by a PLC using algorithms of calculation for the orientation of each element is necessary.

Studies on hemispheric concentrators were conducted, usually to show that they focus at a point just like a paraboloid concentrator (Bellel, 2011). The angle change does not cause a loss in the concentration ratio (Rogers *et al.*, 2012]. Comparisons of the coefficients of concentration with other types of concentrators were also conducted (Bouguetaia, 2013).

We offer a device of hemispheric concentration composed with a receiver constantly in the plan for the least diffusion by manual tracking of the declination.

1. Hemispheric concentrator with crescent receiver: description of the prototype

Figure 2 shows that the sun, in its course from east to west, as reflected on a hemispheric concentrator and creates an image that can be invariably recovered on the crescent receiver.

The section whose projections are recovered is a circle with a radius equal to 0.5 times the radius of the sphere for an angle $\Phi_s = 30^\circ$ which is the half-angle relative to the center of the sphere. The circle moves from west to east at a constant hour angle (Figure 1), and from north to south along the declination (Figure 3) on the hemispheric concentrator. Such a device with its hemispheric concentrator permanently positioned, could concentrate solar

Ky, Thierry S. M., Laboratory of Renewable Thermal Energies, UFR / SEA, 03 BP 7021, University of Ouagadougou, Burkina Faso.

Kam, Sié., Laboratory of Renewable Thermal Energies, UFR / SEA, 03 BP 7021, University of Ouagadougou, Burkina Faso.

Dianda, Boureima, Laboratory of Renewable Thermal Energies, UFR / SEA, 03 BP 7021, University of Ouagadougou, Burkina Faso.

Bathiebo, D. Joseph, Laboratory of Renewable Thermal Energies, UFR / SEA, 03 BP 7021, University of Ouagadougou, Burkina Faso.

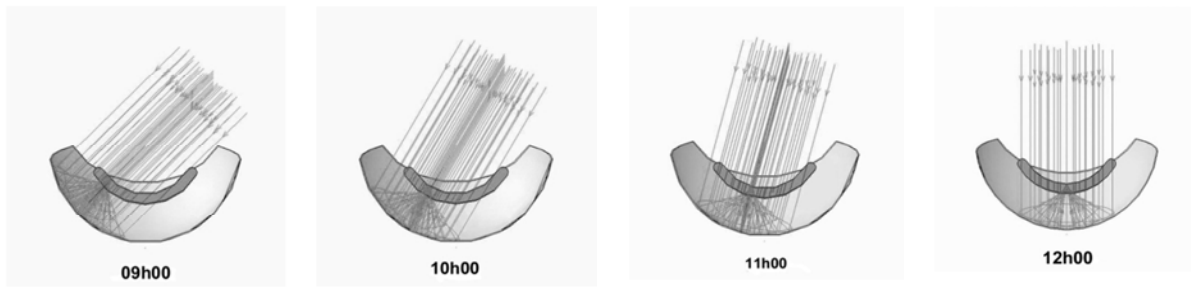


Figure 1: Evolution of the concentration profile with time

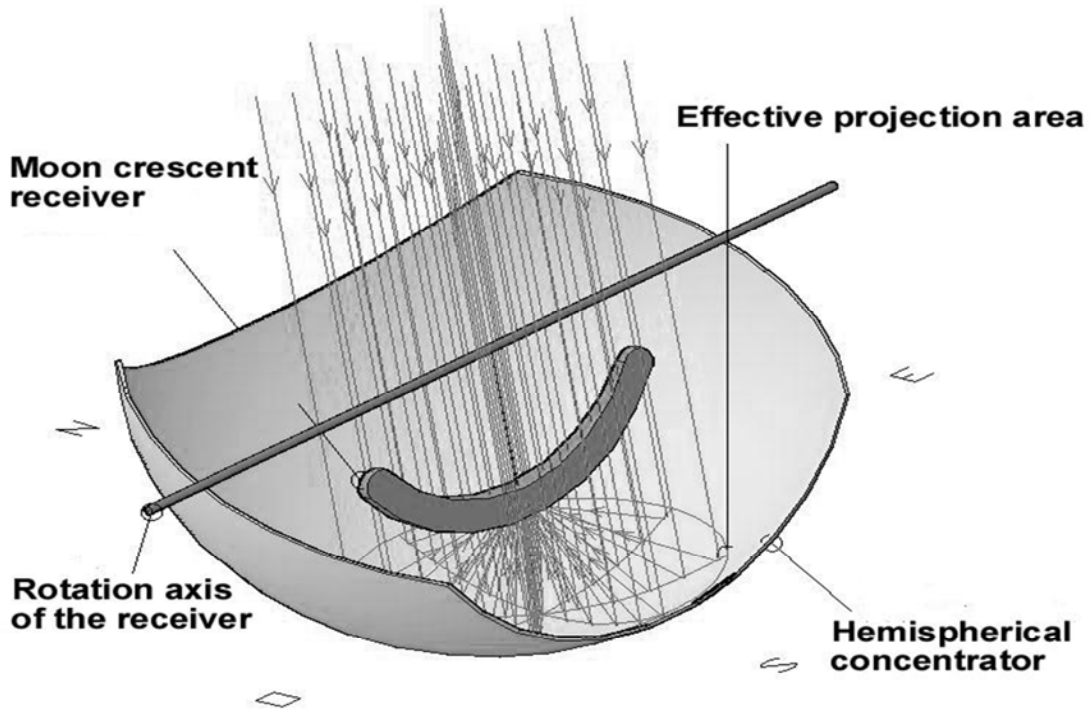


Figure 2: Crescent receiver in the zone for the least diffusion

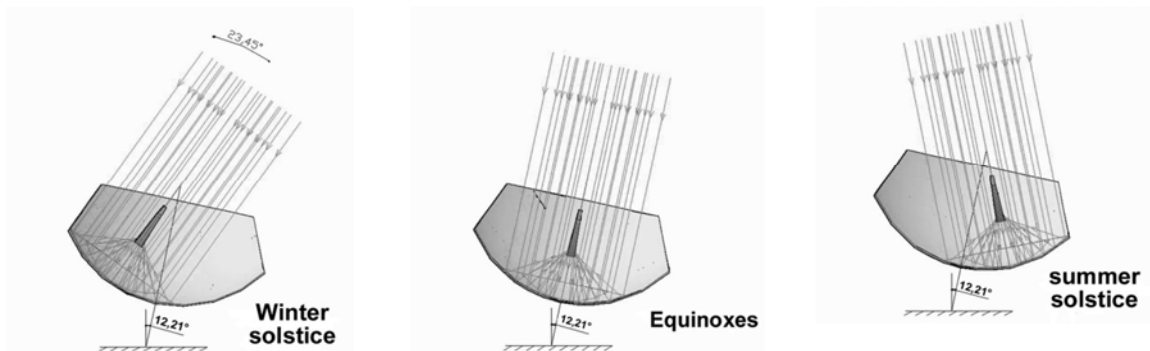


Figure 3: Evolution of the concentration profile with seasons

energy from 8 a.m. to 4 p.m. throughout the year. The receiver is regularly turned on its axis of rotation to less than one degree every three days to follow declination. Thus, in comparison with the Scheffler device, it proves less restrictive because it does not require changing a tilt and a parabolic profile on trial since a simple rotation

of the receiver would be enough. In addition, there is no need for a motorized system of tracking for hour angle. With a possible improvement, the positions of early-month could be shown on a reporter placed at the level of the axis for incremental positions of the receiver during the year.

2. Geometric parameters of a hemispheric concentrator.

The coefficient of geometric mean concentration of the hemispheric concentrator $C_{g_{moy}(Cir_3D)}$ is calculated using the following formula (Bouguetaia, 2013, P.31):

$$C_{g_{moy}(Cir_3D)} = \left[\frac{\sin(2\phi_r)}{\sin \phi_r \sin^2\left(\frac{\phi_r}{4}\right) + 2\theta_s} \right]^2 \dots \dots \dots (1)$$

where ϕ_r is the half-angle describing the width of exposure relative to the focus, and θ_s the top of half-angle reflecting the apparent radius of the sun.

This gives a maximum value of 2964 for an angle $\phi_r = 22^\circ$.

However, to get the value of concentration by this coefficient, we must ensure a proper positioning and sizing of the receiver. The hemispheric concentrator is astigmatic and is considered as a point-concentrator by Gauss approximation only for small-angle values, in comparison with the paraboloid concentrator (Figure 4). The reflections of solar rays are tangent to a surface of revolution called caustic spherical aberration (Figure 5) which has the following Nephroid-type parametric equation (Khaled, 2008, P.55):

$$\begin{aligned} X(\psi) &= r_s \sin^3 \psi \\ Y(\psi) &= \frac{r_s}{2} \cos \psi (1 + 2 \sin^2 \psi) \end{aligned} \dots \dots \dots (2)$$

Where $X(\psi)$ and $Y(\psi)$ are the coordinates of the caustic, r_s is the radius of the hemispheric concentrator and ψ the angle of the Nephroid.

Reflection at point M of the radius corresponding to angle ϕ_s forms a straight line (AM) with equation (Khaled, 2008, P.55):

$$X \cos(2\phi) + Y \sin(2\phi) - r_s \sin \phi = 0 \dots \dots \dots (3)$$

with ϕ , the half angle varying from 0 to ϕ_s .

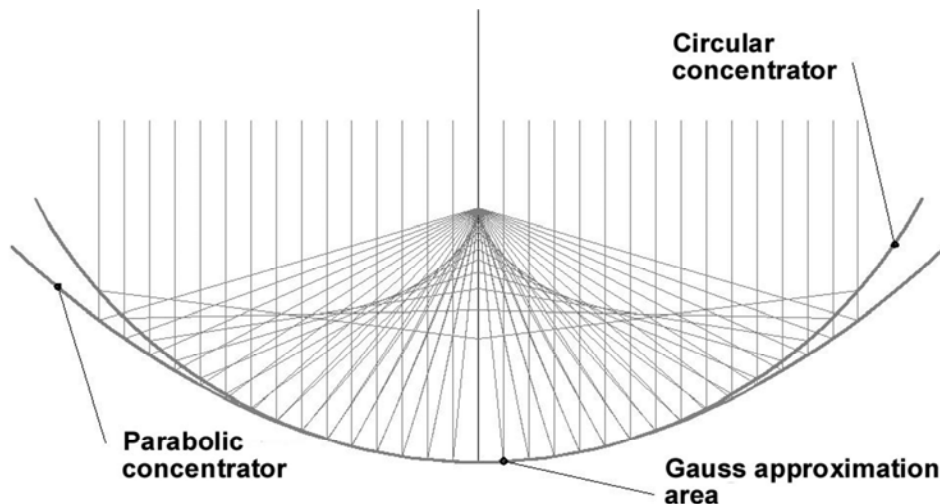


Figure 4: Comparison of the concentration profile of a parabola and a circle

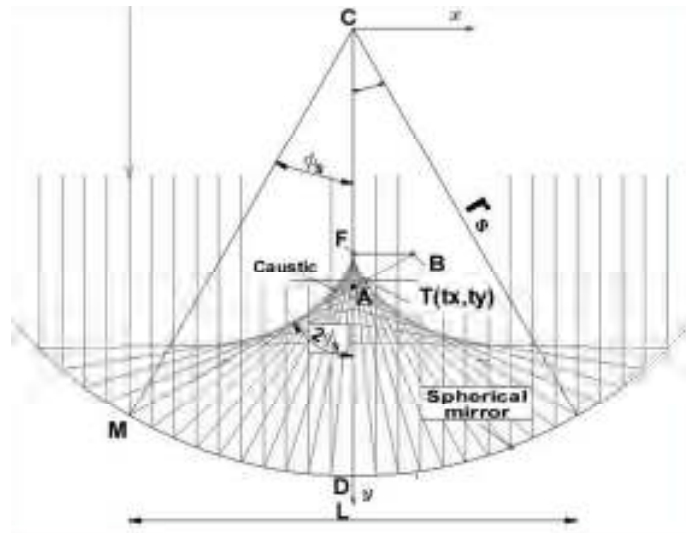


Figure 5: Representation of the caustic and point T (tx, ty) at the plan for the least diffusion

2.1. Position Y(P) of Plan (P) of less diffusion

The intersection of this line with the caustic is done at point T(tx, ty) in which plan (P) of less diffusion is established, a positioning plan of the cavity receiver. We then need to find the point T(tx, ty), which makes it possible to position the cavity receiver on the y axis: Y(P) = \bar{t}_y .

2.2. Radius R_a of the cavity of the receiver

Similarly, to calibrate the receiver, we must know the inner radius R_a of the cavity receiver using the Equations (2) and (3):

$$R_a = \frac{r_s \cos \phi_s - Y_{(p)}}{\cot(2\phi_s + \theta_s)} - r_s \sin \phi_s \text{ with } Y_{(p)} = \bar{t}_y \dots\dots\dots (4)$$

Or :

$$R_a = (r_s \sin \phi_s + r_a) \frac{\cot(2\phi_s)}{\cot(2\phi_s + \theta_s)} - r_s \sin \phi_s \text{ with } r_a = \bar{t}_x \dots\dots\dots (5)$$

2.3. Geometric mean concentration

The geometric mean concentration $C_{g_{mean}(Cir_3D)}^*$ is determined using equation (4) or (5) :

$$C_{g_{mean}(Cir_3D)}^* = \left(\frac{r_s \sin \phi_s}{R_a} \right)^2 \dots\dots\dots (6)$$

The plot of $C_{g_{mean}(Cir_3D)}^*$ is indicated by figure (6). It is observed that the curve has the same shape and the same maximum as that of $C_{g_{mean}(Cir_3D)}^*$ shown in Figure (7) below. In fact, this is the same curve with ϕ_s defined in relation to the center of the hemisphere while ϕ_r is defined in relation to the center of the orifice of the cavity-receiver.

The method used for obtaining point T values (tx, ty) of intersection between the straight line (AM) and the caustic is a numerical approach. It consists to replace the value of X(ψ) and Y(ψ) taken from the parametric equation of the caustic in the equation of the straight line (AM) where ϕ_s is known.

Root ψ_0 of this new equation will give the coordinates of T (tx, ty). (Khaled, 2008, P.56).

$$\sin^3 \psi \cos(2\phi_s) + \frac{1}{2} \cos \psi (1 + 2 \sin^2 \psi) \sin(2\phi_s) - \sin \phi_s = 0 \dots\dots\dots (7)$$

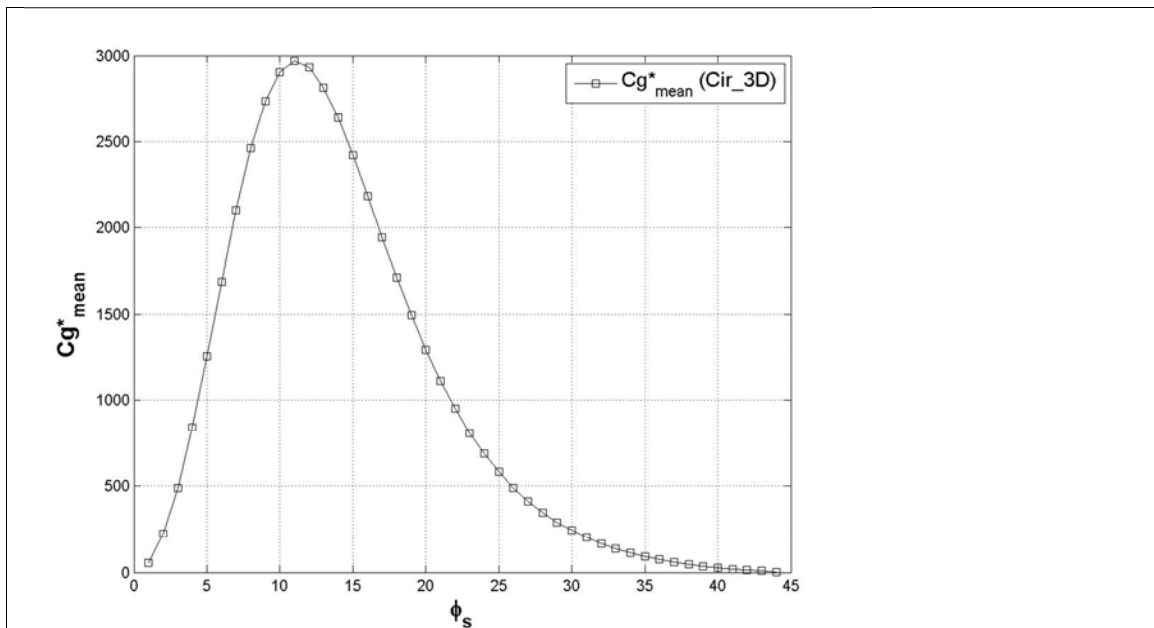


Figure 6: Geometric mean concentration as a function of the angle Φ_s from the centre of the sphere

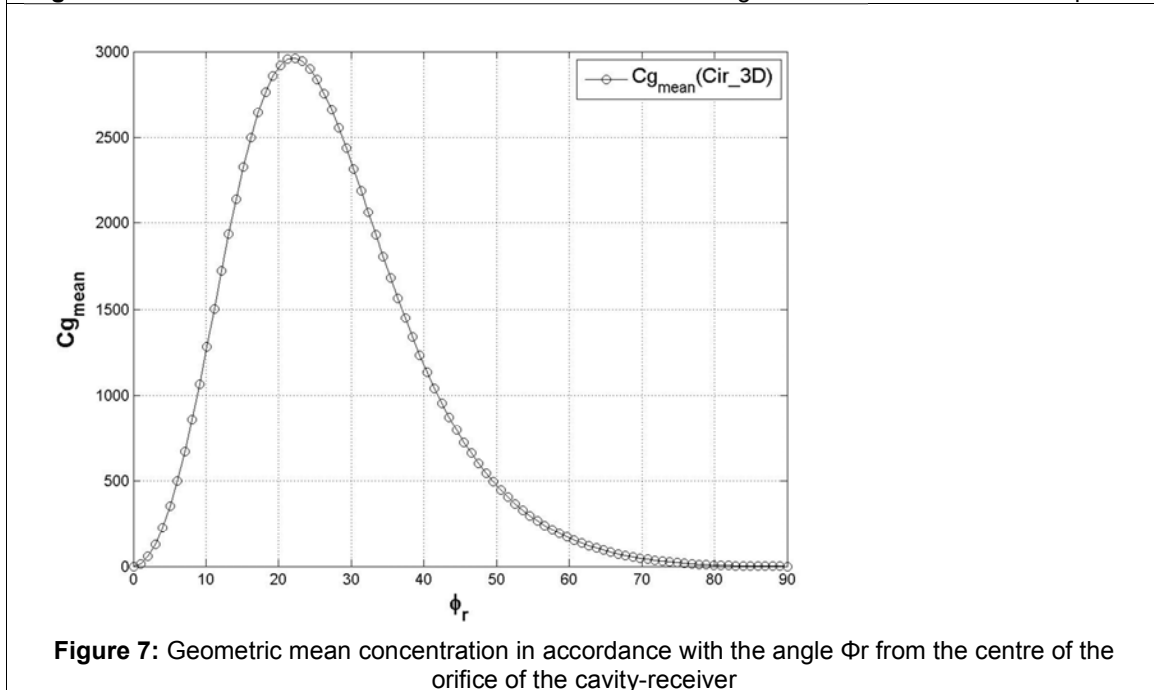


Figure 7: Geometric mean concentration in accordance with the angle Φ_r from the centre of the orifice of the cavity-receiver

It only remains to use an iterative method where ϕ_s can be varied and get the corresponding coordinates of T (tx, ty).

Thereby we obtain the values of ψ_0 as a function of ϕ_s , or $Y(P)/r_s$ according to ϕ_s . These values are indicated in figures (8) and (9).

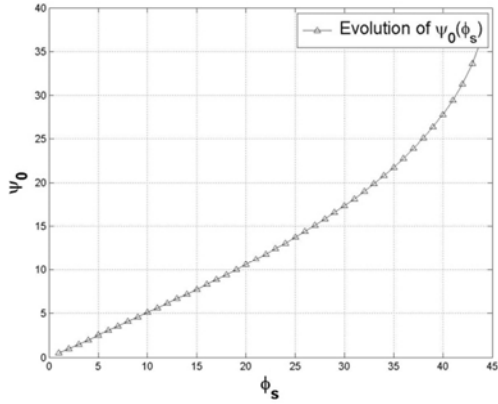


Figure 8: Evolution of the root of the Nephroid ψ_0 with respect to angle Φ_s (in °)

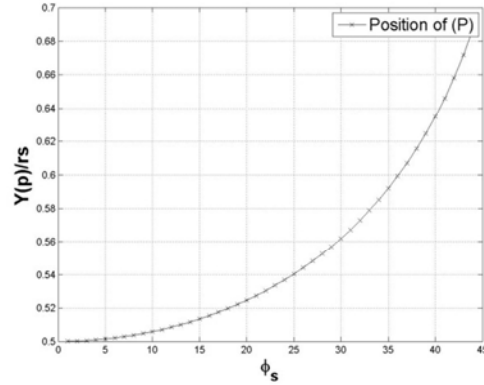


Figure 9: Evolution of the position of the least diffusion plane relative to angle Φ_s (in °)

3. Designing of a collector with a manual tracking system of the declination: Experimental values

The prototype of the study has a truncated hemispheric concentrator made of sheet steel coated on its inside with flat mirror tiles of 5 cm x 5 cm (Figure 10). This results in a dispersion of the radiation that can be quantified by Δ_l (in m):

$$\Delta_l = \frac{0,05}{4} (1 + \sqrt{2}) \dots\dots\dots (8)$$

$$R_a(\Delta_l) = \frac{r_s \cos \phi_s - Y_{(p)}}{\cot(2\phi_s + (\theta_s + \Delta_l))} - r_s \sin \phi_s \quad \text{with} \quad Y_{(p)} = \bar{t}_y \dots\dots\dots (9)$$

Or:

$$R_a(\Delta_l) = (r_s \sin \phi_s + r_a) \frac{\cot(2\phi_s)}{\cot(2\phi_s + (\theta_s + \Delta_l))} - r_s \sin \phi_s \quad \text{with} \quad r_a = \bar{t}_x \dots\dots\dots (10)$$

$R_a(\Delta_l)$ corresponds to the internal radius of the cavity receiver calculated as a function of dispersions Δ_l , it gives a real geometric mean concentration $C_{g_{mean}^*(Cir_3D)}$ calculated using equations (9) or (10):

$$C_{g_{mean}^*(Cir_3D)} = \left(\frac{r_s \sin \phi_s}{R_a(\Delta_l)} \right)^2 \dots\dots\dots (11)$$

$C_{g_{mean}^*(Cir_3D)}$ has a maximum value of 122. This maximum is 4.11% of the previous maximum.

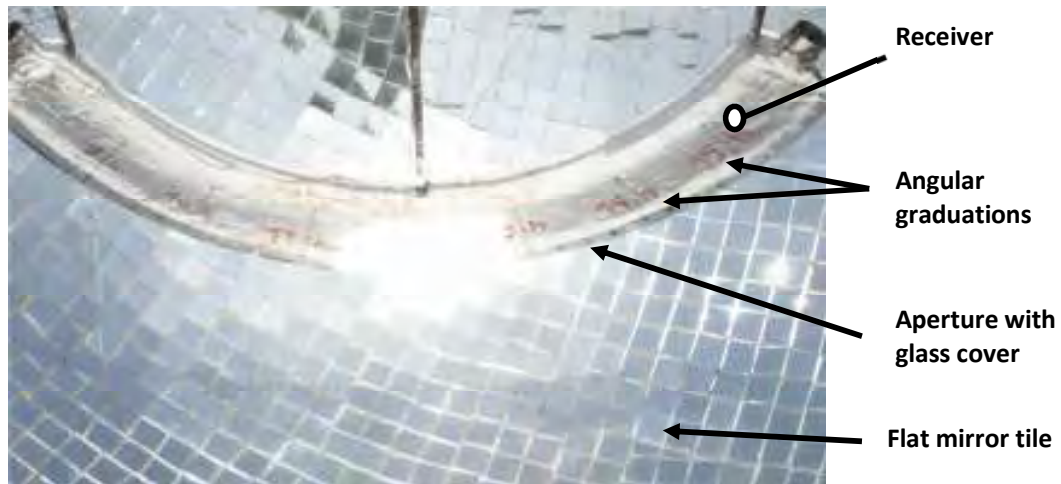


Figure 10: Photo of the prototype: the receiver positioned on the hemispherical concentrator

3.1. Experimental details: studying the device

The prototype (Figure 10) has a radius of 107.3cm for the hemispherical concentrator. The external radius of its receiver is therefore $Y(p)=60.3\text{cm}$. The receiver aperture is $2 * R_a = 7\text{cm}$.

To study the device (Figure 11) the equipment listed below and the related methods of measurement had been used:

- A data logger type Midi LOGGER GL200A and GRAPHTEC brand.

- A probe (probe A) is placed against the glass window of the receiver to measure the temperature in the focal point. To do this, we follow the light spot indicating the reflection of the sun and search for the highest temperature. We got helped by the angular graduations on the receiver, but the precise point was searched around the light spot following the sun's path every 5 minutes.

- A second probe (probe B) reports the ambient temperature.

- A type SL100 and brand KIMO solarimeter is used to measure solar radiation.

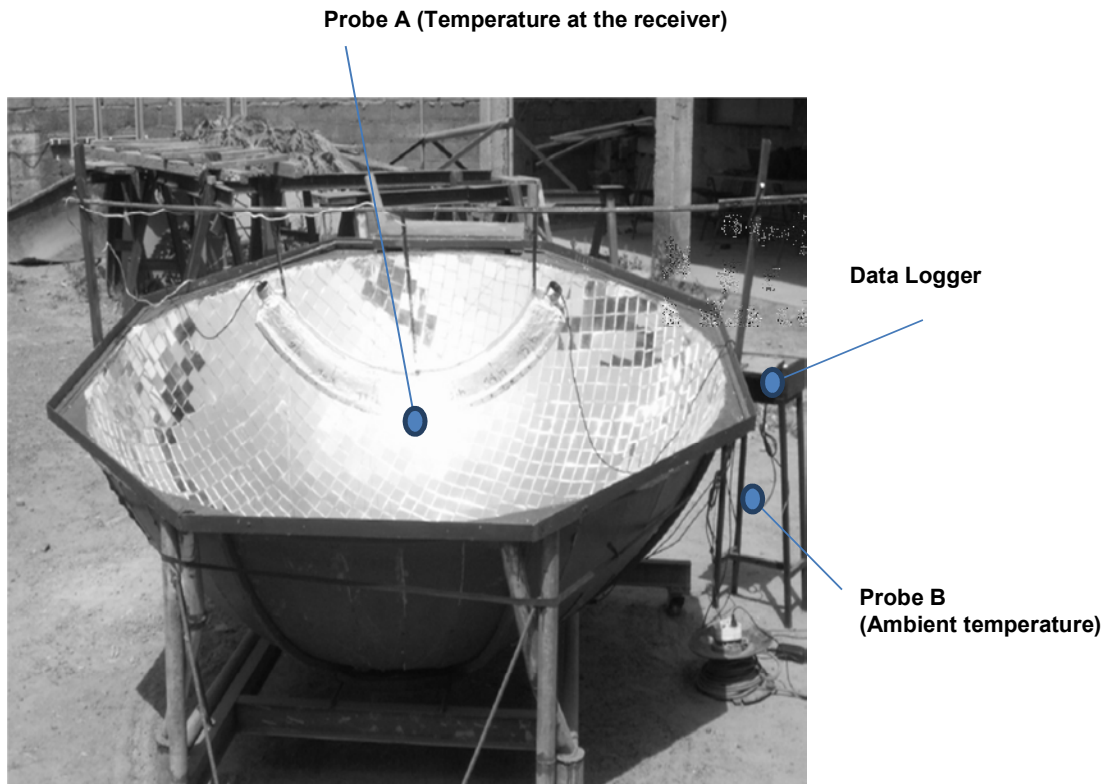


Figure 11: Photo of the device

3.2. RESULTS AND DISCUSSION

We find that the temperature curve for the day of November 07, 2014 (Figure 12) drawn according to surveys at the household level increased gradually until 12.30 p.m. when it reached a peak at 250°C . It roughly follows the evolution of the irradiation of the day (Figure 13). This correspondence is normal, because since the concentration is constant, the temperature is directly a function of the direct irradiation. The few inconsistencies around 12 noon and 1 p.m. are due to cloud-waves.

Another finding also shows that the temperature is already above 120°C as early as 8.30 a.m. and never goes down at any point below this temperature, even at 3 p.m. In short, the temperature ranges between 120°C and 250°C for the whole day.

We find that the temperature curve for the day of December 17, 2014 (Figure 14) drawn according to surveys at the household level gradually increases until it reaches a peak of 260°C at 12 noon. It roughly follows the evolution of the irradiation of the day (Figure 15). This correspondence remains normal because of the constant concentration ratio. The few inconsistencies after 12 noon are due to cloud cover.

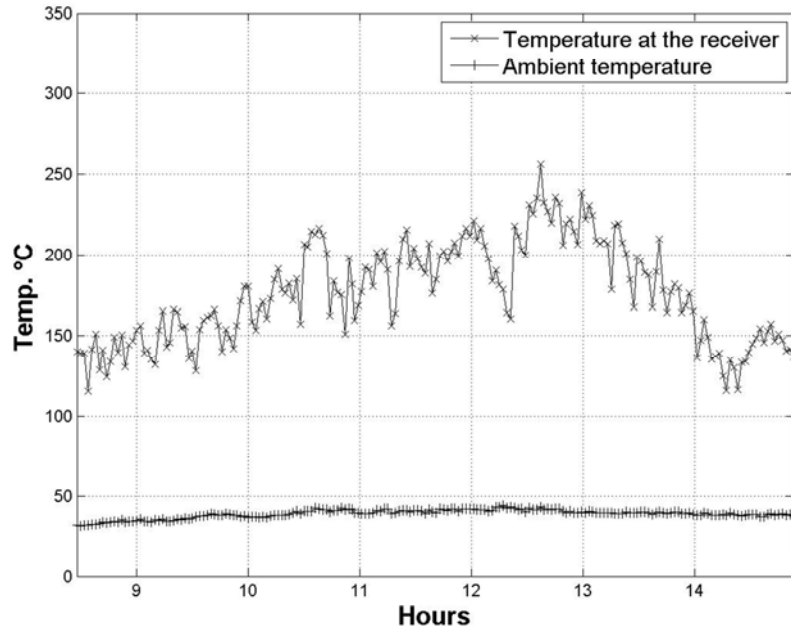


Figure 12: Temperature curves on July 11th, 2014 at $\Phi_s = 30^\circ$

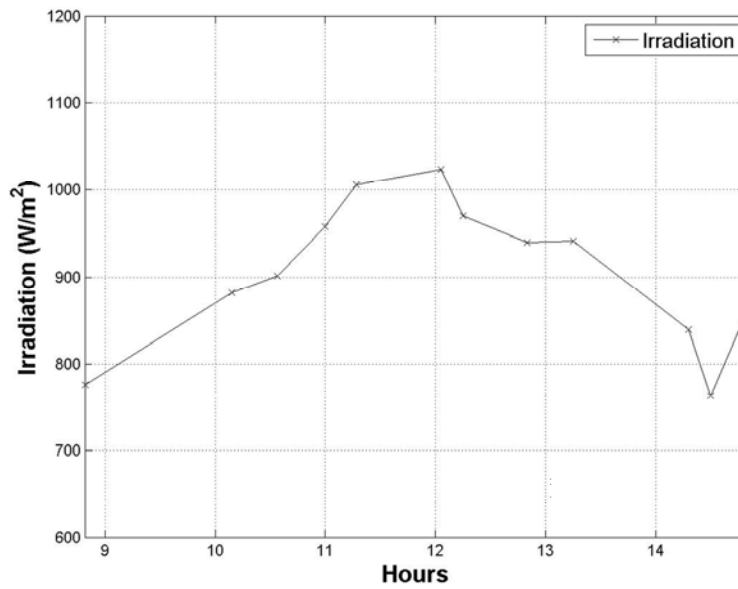


Figure 13: Radiation curve on July 11th, 2014

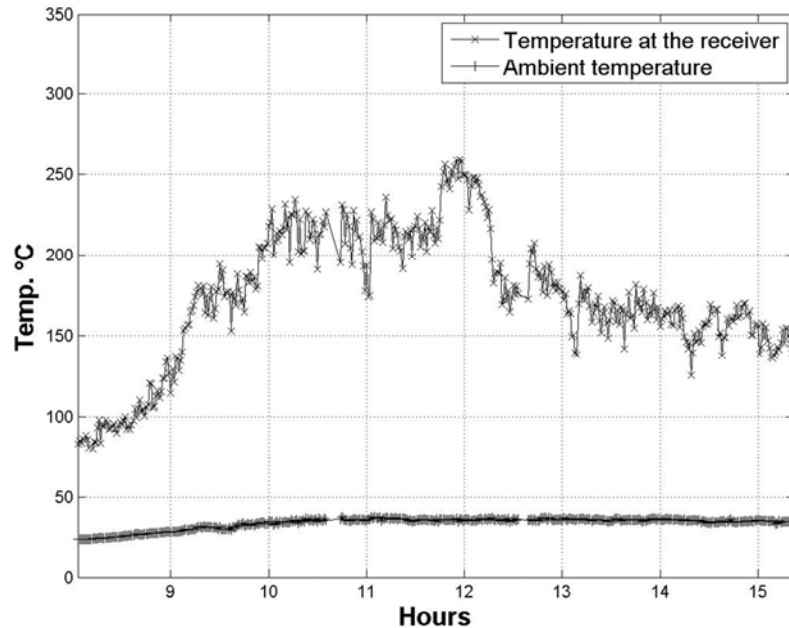


Figure 14: Temperature curves on December 17th, 2014 at $\Phi_s = 22^\circ$

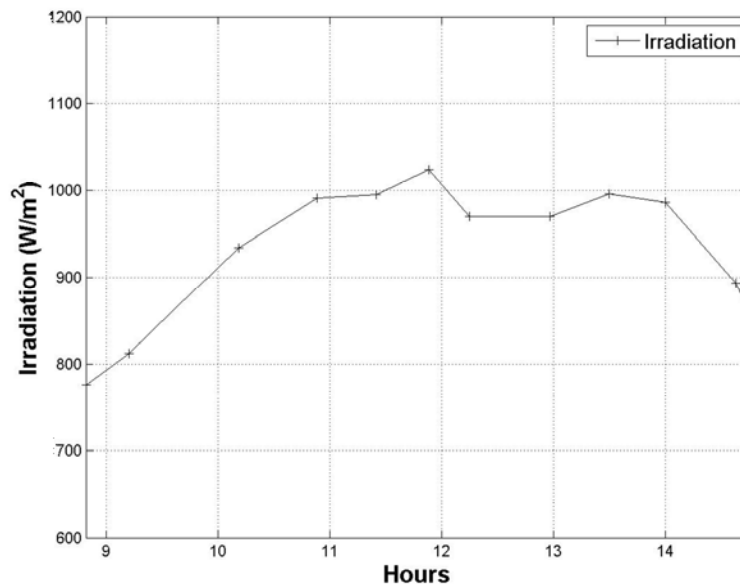


Figure 15: Radiation curve on December 17th, 2014

The temperature remains above 120°C between 9 a.m. and does not go down at any point below this temperature, even at 3 p.m. In short, the temperature ranges between 120°C and 260°C during the day.

The change in Φ_s value from 30° to 22° has nevertheless made hardly noticeable results due to a disrupted afternoon, but there is an increase in the temperature around 200°C at 10 am. This means that despite the fact that the exhibited surface area is reduced for $\Phi_s = 22^\circ$ (from 3.079m^2 to 2.362m^2), the

concentration is better and the temperature also increases accordingly.

CONCLUSION

The study shows that with a hemispheric concentrator having a maximum of geometric mean concentration of 122, it is possible to obtain internal temperatures evolving between 150°C and 260°C from 9 a.m. to 3 p.m. during a day under an average

sunshine of $920\text{W}/\text{m}^2$, with a quasi-fixed tracking system. Such results are obtained with an adjustment on the angle of sun declination only every 2-3 days and a steady hemispherical concentrator. This is much more advantageous than the Scheffler system that is motorized for the tracking of the sun from East to West. In addition, an improvement of these results can be achieved by the rigorous development of the spherical profile of the concentrator (choice of a very smooth wall for the hemispheric concentrator).

Therefore, this prototype of hemispheric concentrator, with the proposed improvements, could advantageously be used for baking bread at temperatures ranging from 250°C to 300°C .

REFERENCES

- Bellel, N., 2011. Study of two types of cylindrical absorber of a spherical concentrator. *Energy precedia* 6: 217-227.
- Bouguetaia, N., 2013. Contribution à l'étude et à la simulation d'un concentrateur cylindro-parabolique. Master's thesis, Université de Constantine 1, Algérie, 94pp.
- Kombassere, A. M. E., 2008. Etude expérimentale des performances thermiques d'un système à concentration à température moyenne. Master's thesis, University of Ouagadougou, Burkina Faso, 44pp.
- Khaled, M., 2008. Conception et réalisation d'un concentrateur sphérique. Master's thesis, Université de Constantine, Algérie, 128pp.
- Munir, A., Hensel, O and Scheffler, W., 2010. Design principle and calculations of a Scheffler fixed focus concentrator for medium temperature applications. *Solar Energy* 84: 1490-1502.
- Quoilin, S., 2007. Les centrales solaires à concentration. Université de Liège, France, 34pp.
- Rogers, S. C., Barichman, C., Chavoor, G., Kinni, M., Glazar, N and Schwartz, P. V., 2012. Concentrating sunlight with an immobile primary mirror and immobile receiver: Ray –tracing results. *Solar Energy* 86 : 132-138.
- Sardeshpande, V and Pillai, I. R., 2010. Effect of micro-level and macro-level factors on adoption potential of solar concentrators for medium temperature thermal applications. *Energy for sustainable development* 16 : 216-223.